

These  $\varphi$ ,  $\psi$  values approximate those found for the helical forms of poly(Pro) and poly(Hyp), and the stabilizing side chain–backbone interaction depicted in III may account for the observation<sup>9</sup> that higher concentrations of  $\text{CaCl}_2$  are required to disrupt the poly(Hyp) helix. It is stressed that this conclusion is tentative, since interaction of the OH and  $\text{C}=\text{O}$  moieties with water molecules or ions may be at least as strong as the proposed  $\text{OH} \cdots \text{O}=\text{C}$  hydrogen bond. The nmr analysis shows only that the Hyp ring assumes the conformation required for formation of an intrachain hydrogen bond. Additional evidence that an increase in stability of helical polypeptide structure results on replacing Pro by Hyp is needed to (a) verify the presence of such bonds and (b) determine the extent that they stabilize, at least locally, a poly(Pro)-type chain conformation.<sup>22</sup>

**Acknowledgments.** I am grateful to Dr. D. Rabenold and Professor L. Mandelkern of the Florida State University

for their gift of the molecular weight characterized sample of poly(Hyp) used in this work and to Mr. R. L. Kornegay of Bell Laboratories for providing the computer program used to simulate the spectrum. The poly(Hyp-Gly) sample was provided by Professor D. F. DeTar of the Florida State University while *tert*-Boc-Gly-Hyp-OH was obtained from Dr. C. M. Deber and Professor E. R. Blout of the Harvard Medical School.

(22) Evidence for Hyp ring–peptide backbone interactions in polypeptides of the form poly(Gly-X-Hyp) would be of particular interest with respect to the role of Hyp in collagen. Pro and Hyp residues in  $\alpha_1$  chains of rat skin collagen occur almost exclusively in triplets Gly-Pro-X and Gly-X-Hyp, respectively, where X is usually not Hyp or Pro.<sup>23</sup> Hence, it is possible for a Hyp residue in the third position to hydrogen bond to the preceding Gly  $\text{C}=\text{O}$ , and stabilize a poly(Pro) type local backbone conformation. It may be noted that in the native collagen molecule a Hyp residue on the second position of the triplet could not perform an analogous function, since the  $\text{C}=\text{O}$  of the third residue in the preceding triplet participates in an interchain hydrogen bond with a Gly NH.<sup>23</sup>

(23) W. Traub and K. A. Piez, *Advan. Protein Chem.*, **25**, 243 (1971).

## Electron Spin Resonance in Crystallizable, High Molecular Weight Polyphenylacetylene<sup>1a</sup>

G. M. Holob,<sup>1b</sup> P. Ehrlich,<sup>\*1b</sup> and R. D. Allendoerfer<sup>1c</sup>

*Department of Chemical Engineering, State University of New York at Buffalo, Buffalo, New York 14214. Received March 14, 1972*

**ABSTRACT:** The thermally activated paramagnetism which appears when crystalline polyphenylacetylene is annealed at successively higher temperatures is introduced irreversibly, if the temperature of the order–disorder transition at about 120° ( $T_c$ ) is not exceeded. Upon cooling below the annealing temperature the esr signal intensity always displays a Curie dependence. A thorough search for triplet spectra was unsuccessful. It is suggested that the unpaired spins are diradicals which originate from  $\pi$  electrons released in the rupture of skeletal  $\pi$  bonds. Although the Curie dependence shows that the paramagnetism does not result from a lattice-independent electronic excitation, the diradicals can be viewed as pairs of “bond-alternation defects” which must have some mobility (Pople and Walmsley).

Studies of electron spin resonance (esr) in polyphenylacetylene prepared by thermal polymerization (PPA-T) and by transition metal catalysts (PPA-C) had established that the paramagnetism of this polymer cannot be associated with a chemical impurity, but must be intrinsic to the molecular structure.<sup>2</sup> The increase in the concentration of unpaired spins per unit sample weight ( $N_s$ ) when freshly prepared PPA-C was heated represented a sharp contrast to the behavior of other conjugated polymers,<sup>3,4</sup> and the change in character of the temperature dependence of  $N_s$  near the temperature where X-ray diffraction indicated an order–disorder transition suggested that at least some of the paramagnetism was associated with irregular chain conformations. Whereas the former phenomenon, *i.e.*, the thermally activated paramagnetism, was consistent with an electronic excitation, the latter indicated the presence of what might be termed “conformational defects.” The structural and dynamic aspects of the two phenomena appeared to be distinct and would, it seemed,

have to be associated with different mechanisms of electronic conductivity.

The “bond-alternation defect” model of Pople and Walmsley,<sup>5</sup> which allows the rapid migration of an electronic excitation, provides perhaps the only mechanism capable of accounting for both electronic conductivity and a thermally activated paramagnetism in polyenes in terms of simple structural concepts. It seemed, initially, that this attractive model would have to be ruled out for PPA, if the paramagnetism were found to be wholly attributable to changes in the electronic properties of the ground state. In either case, it seemed important to determine whether the paramagnetism in PPA was associated with disordered molecules (conformational defects), with electronic excitations, or both, and, if possible, to obtain additional information about the structure of the centers of paramagnetism.

### Experimental Section

The polymer samples used in this study had been obtained by Kern by polymerizing PPA in tetralin in the presence of a rhodium trichloride–lithium borohydride catalyst.<sup>6</sup> PPA prepared with other transition metal catalysts by Kern and also in this laboratory,

(1) (a) Based in part on the Master's thesis of G. M. Holob; (b) Department of Chemical Engineering; (c) Department of Chemistry.

(2) (a) P. Ehrlich, R. J. Kern, E. D. Pierron, and T. Provder, *J. Polym. Sci., Part B*, **5**, 911 (1967); (b) P. Ehrlich, *J. Macromol. Sci.-Phys.*, **2**, 153 (1968).

(3) A. A. Berlin, *J. Polym. Sci.*, **55**, 621 (1961).

(4) M. Nechtschein, *J. Polym. Sci., Part C*, **4**, 1367 (1965).

(5) J. A. Pople and S. H. Walmsley, *Mol. Phys.*, **5**, 15 (1962).

(6) R. J. Kern, *J. Polym. Sci., Part A-1*, **7**, 621 (1969).

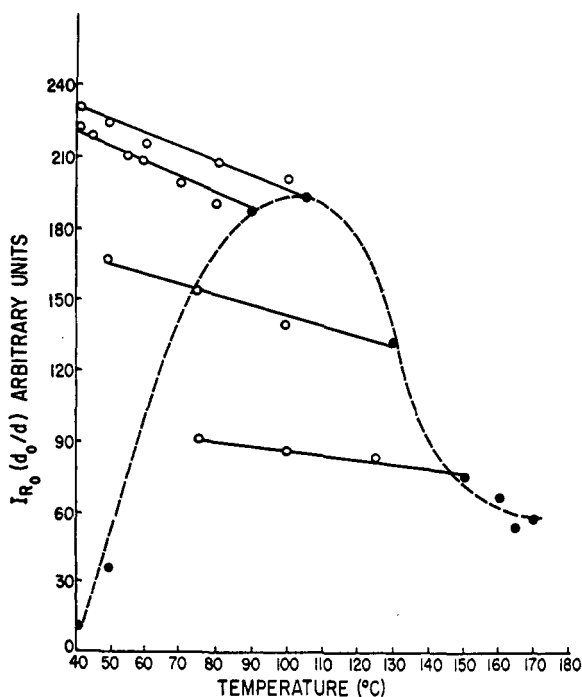


Figure 1. Corrected signal intensity,  $I_{R_0}(d_0/d)$  vs. temperature  $T$  (—) and vs. annealing temperature  $T_A$  (---).

in particular one prepared in the presence of ferric acetylacetonate, all showed the same X-ray diffraction pattern and, at least qualitatively, the same esr behavior.

To eliminate possible contamination by oxygen and to facilitate heat transfer throughout the polymer sample, which in its crystalline form has a low bulk density, the esr sample tubes containing polymer were exhaustively evacuated, flushed, and sealed under a helium atmosphere.

Measurements were carried out on two different spectrometers, a Varian Model 4502 coupled to a  $TE_{011}$  cylindrical cavity and a Varian Model E-9, coupled to a  $TE_{102}$  rectangular cavity. Both instruments were used with X-band detection at a modulation frequency of 100 kcps. The E-9 instrument, having a dynamic range of 60 db, could be used without change in the detector circuit, the 4502 instrument was used in its "low power" configuration only (matched load termination on the reference arm of the bridge). The signal was recorded in its first derivative representation.

Incident power was monitored on a 432-C Hewlett-Packard power meter and the sample temperature was varied by means of a Varian Model E-257 variable-temperature controller.

Calculation of  $T_1T_2$ , the product of the spin-lattice relaxation time  $T_1$  and the spin-spin relaxation time,  $T_2$ , by the continuous-wave saturation method requires knowledge of the average value of the magnetic field intensity,  $H_1$ , which was determined by the method of perturbing spheres.<sup>7</sup> The concentration of unpaired spins was determined by comparison with Varian's 10% KCl in-pitch standard, reported to contain  $3 \times 10^{15}$  spins/cm.

Equilibrium throughout the sample upon increasing the temperature, as tested by a signal which no longer changed with time, was found to take many hours. Under conditions where molecular structure was inferred to change with temperature (see Results), samples were annealed exhaustively in an oil bath at the temperature at which  $N_s$  was to be measured, for a period of 24–48 hr, prior to insertion in the spectrometer. The samples were then kept in the spectrometer for several hours prior to measurement. This procedure was very time consuming but essential in order to determine the conditions under which temperature effects on  $N_s$  were reversible; it was also necessary to follow changes in the bulk density of the

sample by monitoring changes in the sample height within the esr sample tube in order to determine the mass concentration of the unpaired spins.

Density measurements were also carried out for the purpose of obtaining additional information about the transition near 120° by a method of continuous hydrostatic weighing in silicone oil on a temperature-scanning electrobalance.

## Results

At low microwave power, the esr signal always manifests itself as that of a single isotropic species with a near-gaussian line shape. This shape is independent of microwave power, and the peak-to-peak height of the derivative spectrum therefore serves to characterize the concentration of the active species.<sup>2b</sup> Figure 1 represents the data obtained for polymer first annealed at several different temperatures  $T_A$ , and then cooled to temperatures  $T$ . The ordinate  $I_{R_0}(d_0/d)$  represents the peak-to-peak signal intensity, corrected for saturation effects and density changes in such a manner that its product with the absolute temperature becomes proportional to the mass concentration of unpaired spins,  $N_s$ . (If  $I$  represents the peak-to-peak signal height and  $P$  the microwave power,  $I_R = IP^{-1/2}$  and  $I_{R_0}$  represents the limiting value when  $P \rightarrow 0$ , whereas  $d$  and  $d_0$  represent the measured and the reference density, respectively.) The pronounced maximum of the dashed curve near 120° ( $T_c$ ), where the order-disorder transition takes place,<sup>2a</sup> had not been observed earlier,<sup>2b</sup> because of insufficient annealing and failure to allow for changes in bulk density near  $T_c$ . The sharp rise in  $N_s$  with  $T_A$  below 120° is followed by a drop, but a substantial paramagnetism remains in the melt at temperatures well above 220°. (In this and most other conjugated polymers, paramagnetism also exists in solution.<sup>2a,3</sup>) All points on Figure 1, except those corresponding to  $T_A = 40$  and 50°, were obtained from the same sample, annealed at successively higher temperatures. The sample-to-sample reproducibility of given points on the  $N_s$  vs.  $T_A$  curve is not good, and it is possible that this curve is sensitive to the entire thermal history of the sample. The temperature at which the dashed curve displays a maximum occurs at  $120 \pm 10^\circ$ . Within this experimental error, this is the same temperature at which X-ray diffraction data indicate the disappearance of a well-developed crystal structure.<sup>2a</sup>

The maximum on Figure 1 represents a value of  $N_s$  equal to  $1 \times 10^{15}$  spins/g. At a number-average molecular weight of 5000,<sup>2a</sup> this represents about  $10^{-2}$  spin/molecule.

One of the major objectives was to determine whether purely electronic changes could be brought about as a result of temperature changes at essentially constant lattice structure, i.e., whether a reversible electronic excitation, such as a bond-alternation defect, could be detected. To do so  $N_s$  of samples, thoroughly annealed at  $T_A$ , and then cooled to temperatures less than  $T_A$ , had to be determined. The data are represented by the points lying along the solid lines of Figure 1. It was found that the signal intensity changes reversibly upon heating and cooling along these lines.

Inspection of the data suggests that Curie's law may be obeyed ( $I_{R_0}$  proportional to  $1/T$  at constant density,  $N_s$  independent of  $T$ ). The data were analyzed according to the equation  $I_{R_0} = A(1/T) + B$ , and the constants  $A$  and  $B$  were determined according to a least-squares analysis. The results, for several annealing temperatures  $T_A$  are shown in Table I. According to the Curie law,  $B$  must equal zero. We conclude from the moderate standard deviation and the presence of positive as well as negative values of  $B$  that the Curie

(7) E. L. Ginston, "Microwave Measurements," McGraw-Hill, New York, N. Y., 1957.

TABLE I  
ANALYSIS OF TEMPERATURE DEPENDENCE ACCORDING TO  
 $I_{R0} = A(1/T) + B$

$T_A$ , °C	$A \times 10^{-4}$	$B$	$A/T_A$
90	8.5	-46.2	242
105	6.2	+34.5	164
130	6.6	-23.6	151
150	2.7	+12.6	64

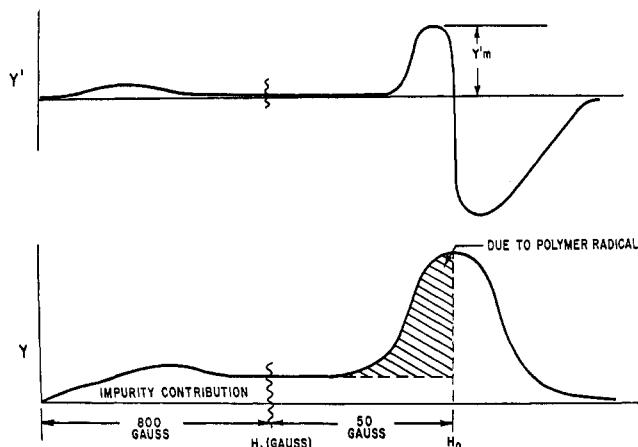


Figure 2. Sketch of esr signal at high power. The derivative curve,  $y'(H_1)$  and the absorption curve  $y(H_1)$ .

law is obeyed. One must conclude that the change in  $N_s$  with  $T_A$  is associated with structural changes in the polymer, whereas the constancy of  $N_s$  with  $T$  indicates the absence of an electronic excitation. The esr signal of PPA then becomes a measure of the concentration of conformationally disordered molecules.

The transition at or near  $T_c$  is not readily detectable by dta measurements, probably because of the low bulk density of the crystalline polymer and the structural collapse at that temperature. This is consistent with a morphology of poorly packed rods.<sup>2a</sup> Although reproducible volumetric data are extremely difficult to obtain on the scanning electrobalance, because readings are largely determined by changes in the bulk morphology, clear changes in density and thermal expansion coefficient occur at 120–135° upon initial heating and disappear eventually after repeated heating and cooling. The data are therefore consistent with an order-disorder transition and the conclusion that one type of long-range order disappears upon adequate annealing at  $T > T_c$ . In the absence of further data, the terms first- or second-order transition are best avoided. Recent measurements have shown that the melting point of the polymer is at least 215°.<sup>8</sup>

Data on the effect of microwave power on signal intensity and line shape allow, under favorable conditions, a determination of the spin-lattice relaxation time  $T_1$ , the spin-spin relaxation time  $T_2$ , and may help to elucidate the structure of the paramagnetic sites. Saturation curves had been determined at low power for concentrated solutions of PPA-T, allowing a calculation of the product  $T_1T_2$ .<sup>2b</sup> By extending measurements to high power levels, an independent determination of  $T_2$  becomes possible.

At increasingly high power, the line shape began to display an asymmetry. This asymmetry, which could eventually be

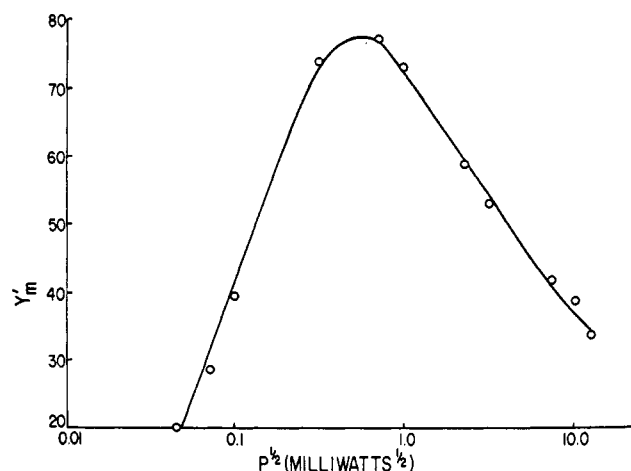


Figure 3. Signal intensity ( $y'_m$ ) vs. square root of microwave power.

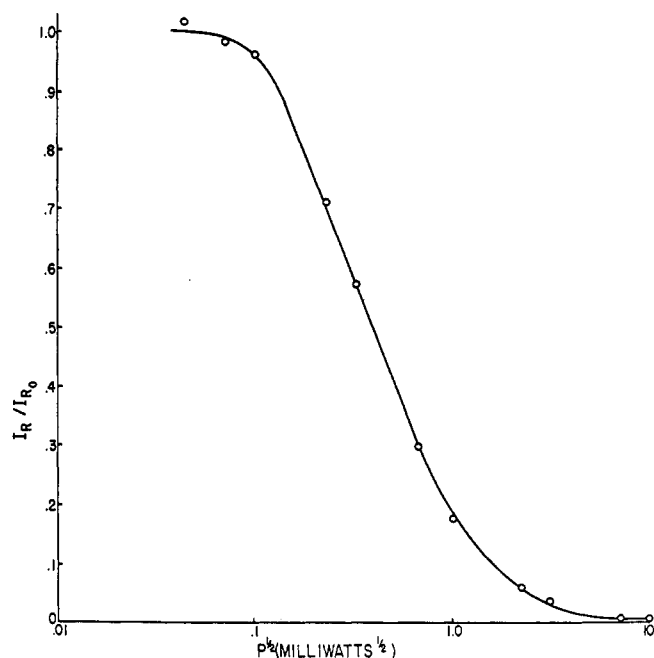


Figure 4. Normalized signal intensity ( $I_R/I_{R0}$ ) vs. square root of microwave power.

attributed to an impurity in the sample tube with a  $T_1$  short compared to that of PPA, was associated with a weak, but broad, absorbance between 2500 and 3000 G. The derivative signal at very high power, and the absorption curve inferred from it, are sketched in Figure 2. If the absorption curve is separated into components due to sample and background in the manner suggested in Figure 2, the low-field peak alone can be made to represent the sample.<sup>9</sup> The line shape of this peak, when analyzed in a manner consistent with Figure 2, was independent of power (or signal asymmetry) in the range investigated. The height of the low-field peak ( $y'_m$  in Figure 2) may therefore be made to represent  $N_s$  after the proper correction for temperature and density effects. (In this case,  $I_R = y'_m P^{-1/2}$ .)

Figure 3 shows a typical plot of the effect of the microwave field on the signal intensity ( $H_1$  proportional to  $P^{1/2}$ ).  $T_1T_2$

(8) B. Biyani, M.S. Thesis, State University of New York at Buffalo, Sept 1971.

(9) C. P. Poole, Jr., "Electron Spin Resonance," Interscience, New York, N. Y., 1967, Chapter 20.

TABLE II  
THE PRODUCT  $T_1T_2$ 

$T_1T_2 \times 10^{12}$ , sec <sup>2</sup>	$P_{1/2}$ , mW	$T$ , °C	$T_A$ , °C
6.10	0.122	22	80
4.92	0.152	40	80
3.86	0.198	80	80
11.95	0.063	22	140
8.30	0.90	80	140
5.17	0.144	110	140
4.24	0.176	140	140

TABLE III  
INDIVIDUAL VALUES OF  $T_1$  AND  $T_2$ 

$T_A$ , °C	$T$ , °C	$\Delta H_{pp}$ , gauss	$a$	$a^a$	$T_2 \times 10^7$ , sec	$T_1 \times 10^5$ , sec
80	-80	13.8	0.025	0.027	1.8	
	22	13.8	0.028			3.5
	40	14.0	0.025			2.8
	80	13.6	0.03			2.2
140	-80	12.1	0.023	0.022	2.5	
	22	12.3	0.02			4.8
	80	11.8	0.021			3.3
	110	12.0	0.021			2.1
	140	12.0	0.023			1.7

<sup>a</sup> Averaged over all  $T$  at fixed  $T_A$ .

is calculated from the value of the field ( $H = H_{1/2}$ ) at the power ( $P = P_{1/2}$ ) at which the normalized signal intensity  $I_R/I_{R_0}$  has dropped to  $1/2$ .<sup>10</sup> One then has  $T_1T_2 = 0.6(\gamma^2 H_{1/2}^2)^{-1}$ , where  $\gamma$  is the gyromagnetic ratio. In the present case the equation reduces to  $T_1T_2 = 7.4 \times 10^{-13}/P_{1/2}$  (rectangular cavity). It is convenient to replot the data in terms of  $I_R/I_{R_0}$  (Figure 4). The values of  $T_1T_2$  obtained in this way for PPA annealed above and below  $T_c$  and measured at several different temperatures are shown in Table II.<sup>11</sup>  $T_1T_2$  is seen to decrease with temperature in the range indicated, and there is an apparent increase with the annealing temperature  $T_A$ . It is impossible to be certain that the latter effect exceeds experimental error. In either case, it is clear that sample crystallinity does not have a large effect on  $T_1T_2$  and, therefore, as will be seen, on  $T_1$ .

The method of Castner<sup>12</sup> allows a determination of  $T_2$  from the asymmetry of curves such as that shown in Figure 3. The method allows a determination of the parameter  $\alpha$  defined by the ratio  $\Delta H_L/\Delta H_{pp}$ , where  $\Delta H_L$  represents the line width of a single lorentzian spin packet and  $\Delta H_{pp}$  the experimentally measured line width between peaks.  $T_2$  is then calculated from  $T_2 = 2(3^{1/2}\gamma\Delta H_L)^{-1} = 1.3 \times 10^{-7}(g\alpha\Delta H_{pp})^{-1}$ , where  $g$  is the  $g$  factor for the free electron. Table III lists values of  $\Delta H_{pp}$ ,  $a$ ,  $T_2$ , as well as  $T_1$ , obtained from  $T_1T_2$  of Table II. It is not certain that the difference for the two samples ( $T_A = 80$  and  $140^\circ$ ) is significant. Assuming it is, the apparent difference in  $T_1T_2$  of samples annealed above and below  $T_c$

(10) N. Bloembergen, E. M. Purcell, and R. V. Pound, *Phys. Rev.* **73**, 679 (1948).(11) A preliminary report of this work (IUPAC Symposium on Macromolecules, Leiden, 1970, p 891) gave values of  $T_1T_2$  whose absolute value was reported incorrectly; the same report also cited data of  $T_1T_2$  obtained below room temperature, with the conclusion that  $T_1T_2$  decreased sharply with increasing  $T$  at low temperature and became constant at  $T > T_c$ . The reexamination of the data carried on here suggests that the latter conclusion should be considered as tentative, since the strong saturation at  $T < \text{room temperature}$  makes the calculation of  $T_1T_2$  quite uncertain, leaving a rather narrow range over which its temperature dependence has been well established.(12) T. G. Castner, *Phys. Rev.*, **115**, 1506 (1959).TABLE IV  
LINE-SHAPE ANALYSIS AND SECOND MOMENTS

$T_A$ , °C	$A/y'_m\Delta H_{pp}^2$			$\langle H^2 \rangle / \Delta H_{pp}^2$			$\langle H^2 \rangle$ (exptl), gauss <sup>2</sup>
	Exptl	G <sup>a</sup>	L <sup>a</sup>	Exptl	G <sup>a</sup>	L <sup>a</sup>	
80	1.17	1.04	3.63	0.29	0.25	$\infty$	55.2
140	1.31			0.36			51.8

<sup>a</sup> G and L stand for gaussian and lorentzian lines, respectively.

could be accounted for by differences in  $T_2$ . In either case, the effect of crystallinity on  $T_1T_2$  is small. The effect of temperature on  $T_1T_2$ , however, is significant and attributable to  $T_1$ .

Little should be inferred at present concerning the mechanism of spin-lattice relaxation from the magnitudes and temperature dependence of  $T_1$  and  $T_2$ . It should be noted, however, that the fact that  $T_1 \gg T_2$  and the temperature behavior observed are consistent with spin relaxation in solids, rather than liquids.

It is of interest to calculate second moments  $\langle H^2 \rangle$  of the derivative curve, since there may be some hope of relating these eventually to electronic structure by means of tractable quantum mechanical models.<sup>13</sup> In addition, the deviation from gaussian line shape may be characterized in terms of the parameter  $\langle H^2 \rangle / \Delta H_{pp}^2$ . The parameter  $A/y'_m\Delta H_{pp}^2$  serves the same purpose, where  $A$  is the area under the absorption curve or the first moment of the derivative curve and  $y'_m$  one-half the peak-to-peak signal height. The results are shown in Table IV. The deviations from a gaussian line shape are seen to be rather small.

A thorough search for a triplet signal was undertaken near the main resonance, at half-field and at intermediate fields at high power levels. No additional resonances, not attributable to the sample tube, could be detected. The apparent asymmetry discussed above led to a renewed search for an anisotropic radical arising from possible interactions with oxygen. The only effect, however, clearly assignable to oxygen, was an increase in signal intensity which could be attributed to a decrease in saturation.<sup>2a,14</sup>

## Discussion

The increase in  $N_s$  with  $T_A$  at  $T_A < T_c$ , its decrease at  $T_A > T_c$ , the Curie behavior upon cooling and reheating at  $T < T_A$ , the identification of the transition at  $T_c$  with an order-disorder process and the retention of the esr signal in solution in approximate proportion to the polymer concentration<sup>2a,8</sup> are all consistent with the hypothesis that the paramagnetism in PPA originates from the  $\pi$  electrons released when skeletal double bonds break, as disordered conformations are assumed increasingly upon increasing  $T_A$  toward  $T_c$ . Some of the more obvious alternate hypotheses, e.g., chemical impurities or loss of hydrogen, are inconsistent with the data presented in this and earlier studies.<sup>2</sup>

It is tempting to associate the transition at  $T_c$  with a disordering of phenyl groups while the conformation of the skeleton remains essentially unchanged. This inference receives some support from model building and calculations<sup>15</sup> which indicate that a cis polymer, severely distorted out of planarity by means of rotations around skeletal single bonds

(13) M. W. Hanna, A. D. McLachlan, H. H. Dearman, and H. M. McConnell, *J. Chem. Phys.*, **37**, 361, 2008 (1962).(14) V. A. Bendersky, B. Y. Kogan, V. F. Gashkovsky, and I. E. Shapnikova, *Karbotsepye Vysokomol. Soedin.*, **253** (1963).

(15) P. Ehrlich, J. Subjeck, and R. G. Rein, unpublished calculations.

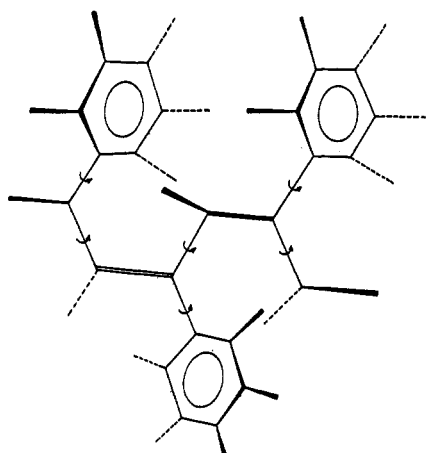


Figure 5. Proposed conformational structure of crystalline polyphenylacetylene.

and chain carbon–phenyl bonds (Figure 5) should be more stable than a  $3^1$  helix based on a trans polymer.<sup>2a</sup> In the cis polymer the phenyl groups are relatively free to assume disordered conformations.

Esr measurements on PPA solutions<sup>2,14</sup> show that, at least in the case of PPA-T,  $N_s$  goes up with molecular weight. If this is true for PPA-C also, then the molecular weight effect and the increase of  $N_s$  with  $T_A$  at  $T_A < T_c$  may both result from a concentration of mechanical energy in  $\pi$  bonds. This suggests in turn that the order–disorder transition is associated with an increase in intramolecular flexibility, which not only prevents further bond breaking at  $T > T_c$ , but even permits partial rehealing of broken  $\pi$  bonds.

One needs to inquire whether line shape and width and the lack of resolution of the hyperfine structure (hfs) permit any inferences regarding the structure of the centers of paramagnetism or the degree of delocalization of the unpaired electrons. Onishi, *et al.*, found a simple unresolved spectrum with a peak-to-peak line width of approximately 17 G in polyenyl radicals obtained by irradiation of several types of polymers, as well as of  $\beta$ -carotene.<sup>16</sup> Furthermore, they found a narrowing of the line toward a limiting width of 13 G by thermal treatment of irradiated poly(vinylchloride). Hanna, *et al.*, on the other hand, studied the esr spectra of polycrystalline samples obtained by  $\gamma$ -irradiation of polyene acids of increasing chain length.<sup>13</sup> The radical obtained from  $\text{CH}_3(\text{CH}=\text{CH})_6\text{COOH}$  did not exhibit hfs, and there is an indication that the second moments may not decrease substantially upon further increase of chain length. Both studies indicate that lack of hfs need not imply electronic delocalization over a chain segment containing more than a few skeletal bonds and that more compounds of defined chemical structure will have to be studied before data on line shape and line width can be used to define further the electronic structure of the paramagnetic conformers in conjugated polymers.

Based on the previous considerations, we propose the following model for the structure of the paramagnetic sites (Figure 6). Rupture of a double bond in the diamagnetic unit A forms paramagnetic unit B, a diradical. By a succession of electronic rearrangements of type 2, unpaired spin density can travel toward the chain ends and become de-

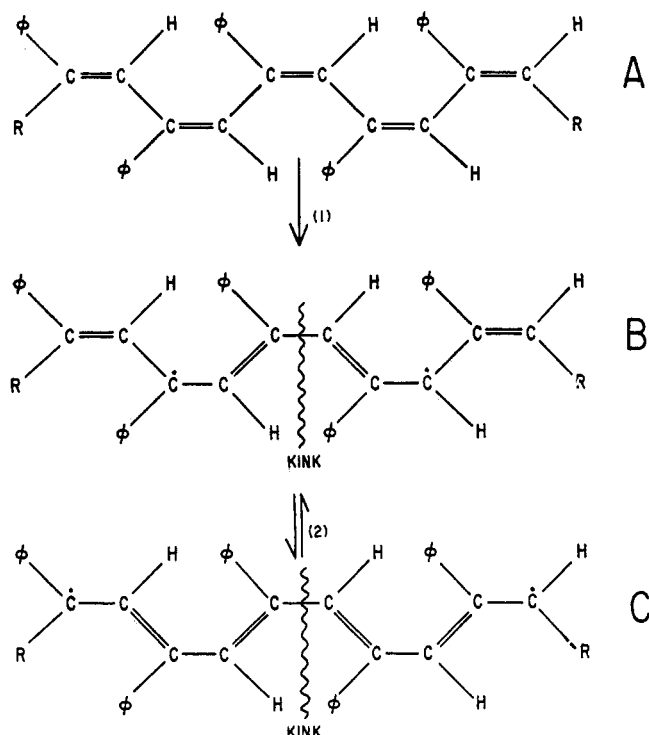


Figure 6. Proposed diamagnetic and paramagnetic ground states of polyphenylacetylene: diamagnetic molecule (A), paramagnetic defect structures (B, C).

localized to a degree consistent with the structure and energetics of the polymer. Structures B and C contain what Pople and Walmsley<sup>5</sup> termed a pair of bond-alternation defects, capable of rapid migration along the skeleton and of providing a mechanism of electronic conductivity. The origin of such "defects" in PPA is, however, different from that proposed by Pople and Walmsley. In their model such defects are purely electronic excitations, associated with the Jahn–Teller effect.<sup>17</sup> In ours, their formation is made possible by a lattice defect, *i.e.*, a ruptured double bond and a kink in the polymer skeleton. A bond-alternation defect thus arises from a conformational defect, and structures B and C, the potentially conducting states, must be viewed as the ground states of defect molecules which, in general, are not in thermodynamic equilibrium with the perfect structure A.

This model probably does not apply to all conjugated paramagnetic polymers. Weill<sup>18</sup> found that exhaustively dehydrohalogenated poly(vinylidene chloride), which approaches the polyene structure, is paramagnetic in the solid state, but not in solution, and he inferred that the paramagnetism was associated with a defect structure brought about by intermolecular, rather than intramolecular electronic rearrangements.

**Acknowledgments.** We appreciate loan of the E-9 spectrometer by Professor D. J. Kosman, Department of Biochemistry. We also acknowledge gratefully support of this research by the National Science Foundation through Grant No. GK-3998 and by the State University of New York through award of a faculty fellowship to one of us (P. E.)

(17) L. Salem, "The Molecular Orbital Theory of Conjugated Systems," W. A. Benjamin, New York, N. Y., 1966, Chapter 8.

(18) G. Weill, Centre de Recherches sur les Macromolécules, Strasbourg, personal communication.

(16) S. Onishi, Y. Ikeda, S. Sugimoto, and I. Nitta, *J. Polym. Sci.*, **47**, 503 (1960).